Spectrochimica Acta Part A: Molecular and Biomolecular Spectroscopy 257 (2021) 119761

Contents lists available at ScienceDirect

Spectrochimica Acta Part A: Molecular and Biomolecular Spectroscopy

journal homepage: www.elsevier.com/locate/saa

Colorimetric assay based on horseradish peroxidase/reduced graphene oxide hybrid for sensitive detection of hydrogen peroxide in beverages

Fatemeh Behrouzifar [a], Seyed-Ahmad Shahidi [a], Fereshteh Chekin [b,*], Shabnam Hosseini [c], Azade Ghorbani-HasanSaraei [a]

[a] Department of Food Science and Technology, Ayatollah Amoli Branch, Islamic Azad University, Amol, Iran
[b] Department of Chemistry, Ayatollah Amoli Branch, Islamic Azad University, Amol, Iran
[c] Department of Material Science and Engineering, Ayatollah Amoli Branch, Islamic Azad University, Amol, Iran

HIGHLIGHTS

- We report a colorimetric assay for detection of H_2O_2 based on the oxidation ABTS.
- The rGO was prepared using the green tea extract agent and decorated by HRP.
- H_2O_2 can be catalysed by HRP-rGO and converted into water and oxygen.
- The detection limit of analysis was ≈15 nM.
- Also, the biosensor was adapted to monitor H_2O_2 in different beverages.

GRAPHICAL ABSTRACT

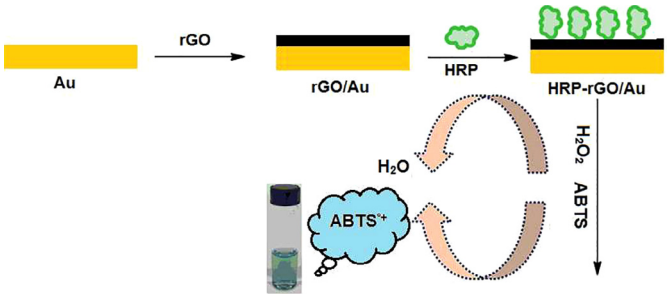

ARTICLE INFO

Article history:
Received 16 January 2021
Received in revised form 22 March 2021
Accepted 27 March 2021
Available online 31 March 2021

Keywords:
Hydrogen peroxide
Green tea extract
Horseradish peroxidase
Reduced graphene oxide

ABSTRACT

We reported a simple and sensitive colorimetric assay for detection of hydrogen peroxide (H_2O_2) based on the oxidation of 2,2′-azino-bis(3-ethylbenzothiazoline-6-sulfonic acid) (ABTS) by UV–Vis spectroscopy method. The reduced graphene oxide (rGO) was prepared using green tea extract as bio-reducing and stabilizer agent and decorated by horseradish peroxidase (HRP). The surface of Au interface was modified with HRP-rGO hybrid. The formation of HRP-rGO hybrid was confirmed by cyclic voltammetry, scanning electron microscopy (SEM), energy-dispersive X-ray Spectroscopy (EDX) and Raman spectroscopy·H_2O_2 can be catalysed by HRP-rGO hybrid and converted into water and oxygen. The ABTS substrate takes up oxygen to form a green coloured product that has absorption peaks at 421, 655 nm and 737 nm. The colour development is linearly dependent on HRP in the range of 4–50 μg/L. The color of the green product solution is stable for 20 min. The absorption intensity is strongly related to the hydrogen peroxide concentration. The absorption intensity of the formed product scaled linearly with the hydrogen peroxide concentration in the ranges of 0.3–20 μM and 20–8000 μM with a detection limit of ≈15 nM could be achieved. The biosensor with excellent limit detection and wide linear ranges was adapted to monitor H_2O_2 in different beverages.

* Corresponding author.
E-mail address: fchekin@gmail.com (F. Chekin).

https://doi.org/10.1016/j.saa.2021.119761
1386-1425/

1. Introduction

Hydrogen peroxide (H_2O_2) as mediator and oxidizing agent [1] is used in different fields such as food industries, clinical, pharmaceutical and environmental [2,3]. H_2O_2 is a byproduct in metabolic oxidation processes. When H_2O_2 concentration reaches 75 ppm, it is dangerous to life and health [4]. The excessive amount of H_2O_2 can cause the physiological and pathological events such as Alzheimer, Parkinson, amyotrophic lateral sclerosis, cancer, traumatic brain injury, ischemia/reperfusion injury, impaired learning and memory functions [5,6]. So, the simple, highly sensitive, low-cost and rapid detection of hydrogen peroxide has been particularly important and widely studied. The several analytical methods including spectrophotometric, titrimetry, chemiluminescent, fluorometric, high performance liquid chromatography (HPLC) and electrochemistry were reported for low levels determination of H_2O_2 [7–18]. The most of them require expensive reagents and instruments, skilful techniques and complicated procedures. The peroxidase-based interfaces are useful to effective detection of H_2O_2 [19]. Among peroxidases, horseradish peroxidase (HRP) has long been a representative enzyme to investigate the structure, dynamic and thermodynamic properties of peroxidases, particularly to explore the biological behavior of H_2O_2 catalyzed oxidation. The HRP is a heme-containing oxidoreductase used in diagnostics for a wide range of applications. The detection principle is related to the oxidation or reduction of a substrate under the catalysis of a natural enzyme. The change of color or signal intensity is linear with the target concentration [20]. In the 2,2′-azino-bis(3-ethylbenzothiazoline-6-sulfonate) (ABTS)-HRP systems, the measurement is based on the consumption of H_2O_2 by peroxidase in the presence of ABTS. ABTS regenerates peroxidase giving a radical-cation (ABTS·+) with an absorption maximum at 414 nm, the intensity which is proportional to the amount of H_2O_2 present in the sample [21].

The establishment of a simple strategy for stable enzyme immobilization on platform is important to develop biodevices. Conventional methods of enzymes immobilization include covalent binding, physical adsorption, encapsulation in polymers, and cross linking to a suitable supporting matrix [22]. Among various enzyme immobilization methods, physical adsorption is one of the easiest methods and can be performed under relatively mild conditions. HRP is easily denatured through the direct adsorption of HRP onto a bare surface and results in bioactivity loss [23]. Furthermore, physical adsorption results in a lack of operational and stability. Various functional materials including self-assembled monolayer (SAM), catalysts and proteins have been utilized to modify the surface of platform to construct bio-devices [24,25].

The use of nanomaterials for the development of bio-devices has aroused considerable interest. Graphene and its derivatives (e.g., graphene oxide (GO) and reduced graphene oxide (rGO)) are a single layer of carbon atoms with a two-dimensional honeycomb sp^2 carbon lattice [26–29]. Graphene-based materials have shown great promise as high-performance matrices for enzyme immobilization [30–32], offering advantages such as large surface area, tailor-made surface functionalities and easy substrate accessibility [33,34]. The type and distribution of surface functionalities of nanomaterial affect the interactions between nanomaterial and enzymes and consequently, the structural conformation and substrate accessibility to adsorbed enzymes. Also, hydrophobic effects are the predominant mechanism for the adsorption of enzyme on rGO [35]. Different interactions between enzyme and nanomaterial had different effects on substrate accessibility to the heme, resulting in an increase or a decrease in enzyme activity [36]. This study was undertaken to develop a HRP-rGO/Au biosensor to measure hydrogen peroxide concentration in the presence of ABTS (Fig. 1). Furthermore, conditions for the colouring of ABTS by HRP-rGO/Au and hydrogen peroxide were optimized.

2. Experimental

2.1. Materials

The green tea used in this study was prepared from the local market of Rasht city. Potassium hexacyanoferrate(II) ($[K_4Fe(CN)_6]$), potassium chloride (KCl), 2,2′-azino-bis(3-ethylbenzothiazoline-6-sulfonate) (ABTS), horseradish peroxidase (HRP), N-hydroxysuccinimide (NHS), N-ethyl-N-(3-dimethylaminopropyl) carbodiimide (EDC), hydrogen peroxide (H_2O_2), phosphoric acid (H_3PO_4), sodium dihydrogen phosphate (NaH_2PO_4), disodium hydrogen phosphate (Na_2HPO_4) and sodium phosphate (Na_3PO_4) were purchased from Sigma-Aldrich and used as received. Graphene oxide (GO) was purchased from Iranian Nano Materials Pioneers. The different beverages were purchased from the local market (Amol, Iran).

2.2. Apparatus

Electrochemical experiments were performed with a potentiostat/galvanostat (Sama 500-c Electrochemical Analysis system, Sama, Iran) using a three-electrode system consisting of Ag|AgCl|KCl_{3M} as the reference electrode, HRP-rGO modified carbon paste electrode as working electrode and platinum wire as auxiliary electrode. UV–Vis tests were recorded by UV–Vis spectrophotometer (UV-1900, Shimadzu Co., Japan). Raman analysis was performed with a Takram P50C0R10 Raman spectrometer (Teksan, Iran) containing CCD array detector and a laser (532 nm). FE-SEM images were obtained by an electron microscope (MIRATESCAN-XMU, Czech Republic) combined with energy-dispersive X-ray (EDX) machine equipped with three detectors and a thermal field emission emitter.

2.3. Preparation of reduced graphene oxide

The reduced graphene oxide (rGO) was prepared based on previous report [37]. To obtain green tea extract, green tea (3 gr) in 25 mL of distilled water was sonicated for 45 min at 50 °C and the extract was isolated by filtration. 20 mL of green tea extract was added drop by drop to 20 mL of GO aqueous suspension (0.5 mg/mL). Then mixture was refluxed for 8 h at 60 °C. The product (rGO) was precipitated and isolated by centrifugation (15000 rpm) for 15 min. At least, rGO was washed with water and dried in an oven at 60 °C overnight.

2.4. Fabrication of HRP-rGO modified electrode

The carbon paste electrode (CPE) was prepared based on previous report [38]. Breifly, the paraffin was added drop by drop to 0.5 gr of graphite powder and hand-mixed until a uniformly wetted paste was obtained. Then the carbon paste was packed into a glass tube with internal radius 3 mm and a copper wire was used to electrical contact. The polishing of glass tube was carried out on weighing paper.

1 mg of rGO in 1 mL of water was sonicated for 40 min. 5 μL of this solution was drop-casted onto the CPE and allowed to dry in an oven at 60 °C. Then, 5 μL of the HRP solution (5 mg/mL) was deposited on the surface of rGO/CPE, and adsorption of the HRP was allowed to proceed overnight at 4 °C. The HRP-rGO/CPE was washed with buffered phosphate solution (PBS, 0.1 M and pH 7.4) and used for electrochemical tests.

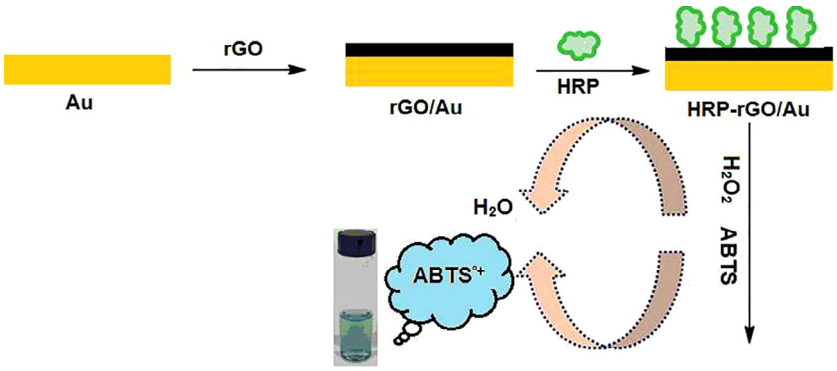

Fig. 1. Schematic illustration for the preparation HRP-rGO modified Au as biosensor for detection of hydrogen peroxide.

2.5. Preparation of HRP-rGO modified interface

The Au interface was immersed into cysteine (1 mM) for 2 h at room temperature. 10 μL of rGO aqueous suspension (1 mg/mL) was drop casted on Au by first activating the carboxyl groups via immersion into a solution of EDC (10 mM) and NHS (10 mM) in PBS (0.1 M, pH 7.4) for 45 min. 8 μL of the HRP solution (5 mg/mL) was deposited on the surface of rGO/Au interface, which was then placed in a petri dish, and adsorption of the HRP was allowed to proceed overnight at 4 °C. The HRP-rGO/Au interfaces were thoroughly rinsed with PBS solution (0.1 M, pH 7.4), and if not used immediately they were stored at 4 °C.

2.6. Colorimetry experiments

1 mg of ABTS was added into PBS solution 0.1 M (pH = 7.4, 2 mL), followed by the addition of H_2O_2 (30%, 5 μL) and immersion of HRP-rGO/Au interface into solution. The UV/Vis spectra were recorded at 421 nm after reaction for 10 min to form a green soluble product vs. a blank containing only the PBS solution. All assays were done at 25 °C.

2.7. Analysis of real samples

500 μL of different beverages were added into 5 mL of PBS solution 0.1 M (pH = 7.4) containing 1 mg ABTS. Then, the certain amounts of H_2O_2 were added to solution and were analysed by UV–Vis at 421 nm after 10 min.

3. Results and discussion

3.1. Characterization

The morphology of rGO and HRP-rGO is characterized with FE-SEM. As seen in Fig. 2, the rGO is a wavy shape and thin layers (Fig. 2a). In contrast, the image of HRP-rGO (Fig. 2b) shows that rGO sheets is decorated by flower-like HRP. This observation confirms the formation of HRP-rGO hybrid. The EDS pattern shown in Fig. 2c indicates that the rGO contains only C and O elements, while the EDX spectrum of HRP-rGO (Fig. 2d) contains C, O and Fe elements. This result confirms the formation of HRP-rGO hybrid.

Raman analysis of rGO and HRP-rGO was also performed (Fig. 3) and revealed the introduction of defects in the graphene framework after decoration of rGO by HRP. The D and the G bands of rGO are appeared at 1326 cm^{-1} and 1601 cm^{-1} with the intensity ratio of D and G bands (I_D/I_G) of 1.9. The D and G bands of HRP-rGO are shifted to 1368 cm^{-1} and 1619 cm^{-1}, and the I_D/I_G of HRP-rGO is calculated to be 0.85. The I_D/I_G of rGO decreased after the introduction of HRP on rGO. It represents that not only there is physical adsorption of HRP on rGO nanosheets but also HRP interacts chemically with rGO. Also, D and G bands of HRP-rGO shift due to decrease the number of free functional groups indicating the deformation of ordered structure and the appearance of different groups.

Furthermore, the electrochemical behavior of rGO and HRP-rGO interfaces was also monitored using $[Fe(CN)6]^{3-/4-}$ as the redox couple by cyclic voltammetric. As shown in Fig. 4, the redox current decreased in the presence of HRP-rGO. The COOH, N and Fe groups of HRP were used for the integration to rGO. Covalent integration of the HRP results in further decrease in charge transfer due to the formation of an insulating barrier. Moreover, the presence of HRP decreases the active sites and electrical conductivity of rGO. The active surface area of rGO/CPE and HRP-rGO/CPE was determined by $[Fe(CN)_6]^{4-}$ (5 mM) from the slope of plotting the peak current vs. the square root of the scan rate using Eq. (1) [39]:

$$A = \text{slope} / \left(268.6 \times n^{3/2} \times D^{1/2} \times C\right) \quad (1)$$

where A, n, D and C are the active surface area (cm^2), number of transferred electrons (n = 1), diffusion coefficient of $[Fe(CN)_6]^{4-}$ and concentration of $[Fe(CN)_6]^{4-}$, respectively. In contrast to rGO/CPE (0.136 cm^2), HRP-rGO/CPE shows a decreased surface area (0.091 cm^2).

3.2. UV–Vis experiments

Fig. 5 shows the UV–Vis spectrum of a solution of ABTS (1 mg) and H_2O_2 (30%, 5 μL) in PBS (2 mL, pH 7.4) after immersion of HRP-rGO/Au for 15 min. As seen, the absorption peaks became apparent at 421 nm, 655 nm and 737 nm that the UV–Vis measurements were recorded at strong band of 421 nm. Also, the effect of time in catalytic reaction by HRP is shown in Fig. 6a. As shown, the catalytic reaction was completed after 10 min, the color and absorbance of solution is approximately constant in range of 10–20 min and is decreasing after 20 min. So, 10 min reaction time was chosen as optimum time for recording UV–Vis spectra.

Fig. 6b shows the effect of rGO in HRP amount immobilized on Au interface. As observed, the absorption of solution after immersion of HRP-rGO/Au interface in solution of PBS (2 mL, pH 7.4) containing ABTS (1 mg) and H_2O_2 (30%, 5 μL) is higher than immersion of HRP/Au in the same solution. It's found, rGO because of large surface area, tailor-made surface functionalities and easy substrate accessibility shows as high-performance matrices for HRP immobilization. Also, hydrophobicity of rGO effects the adsorption of HRP on rGO [35].

The concentration of active HRP immobilized onto rGO/Au biosensor for determination of H_2O_2 was optimized by using the HRP different concentrations recorded in Fig. 6c. The experiment was done by keeping the concentrations of ABTS (1 mg) and H_2O_2 (30%, 5 μL) in PBS (2 mL, pH 7.4), whereas the HRP-rGO/Au

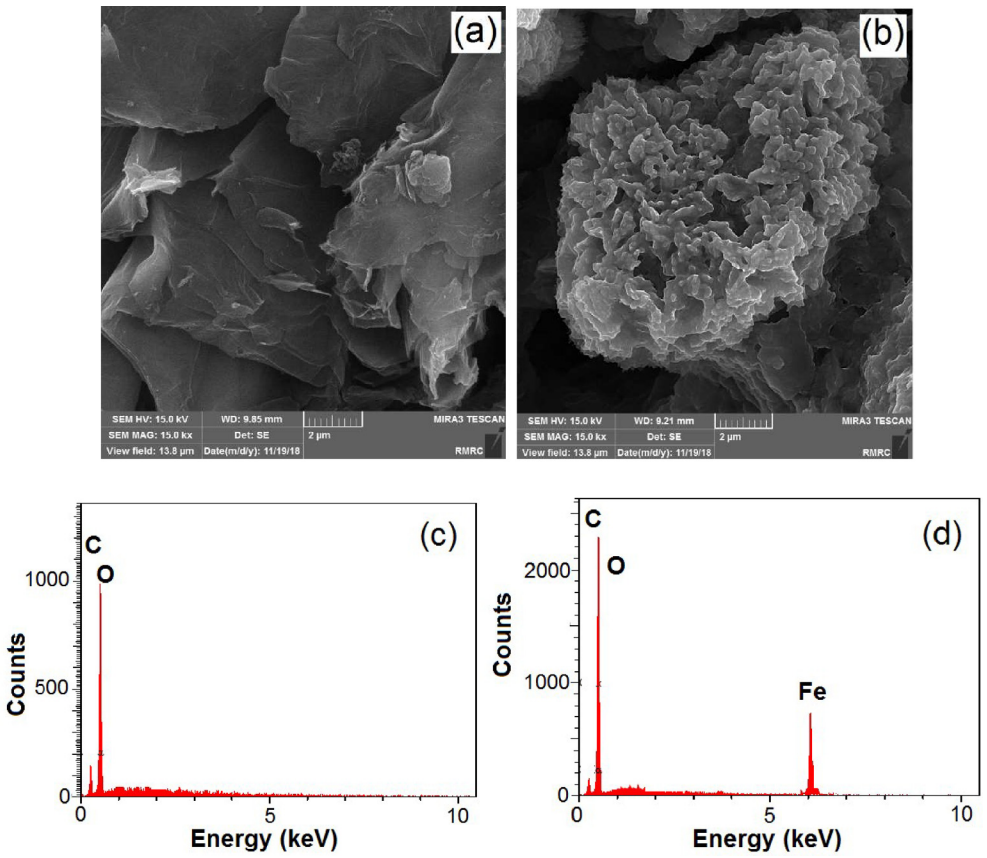

Fig. 2. FE-SEM images of rGO (a), HRP-rGO; EDX of rGO (e) and HRP-rGO (f).

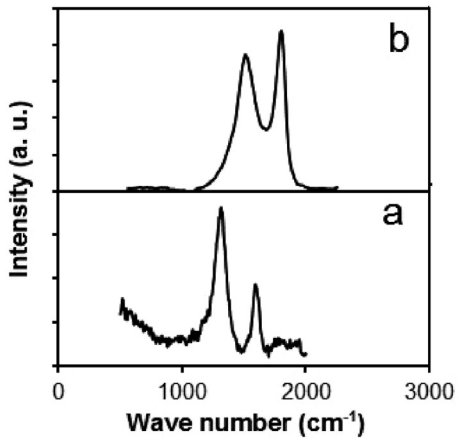

Fig. 3. Raman spectra of rGO (a) and HRP-rGO (b).

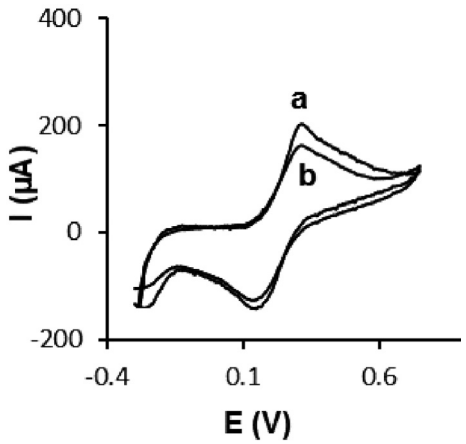

Fig. 4. Cyclic voltammograms of (a) rGo/CPE and (b) HRP-rGO/CPE in 0.1 M PBS (pH 7.4) and scan rate of 100 mV s^{-1}.

biosensors immersed in the solution have different amount of immobilized HRP. As from the absorption maximum seen in, the active HRP concentration corresponds to 50 μg/L.

3.3. Determination of hydrogen peroxide

The HRP modified rGO/Au biosensors were used to determine hydrogen peroxide in solution of PBS (2 mL, pH 7.4) containing ABTS (1 mg) by UV–Vis spectroscopy (Fig. 7a). H_2O_2 was added in different concentrations to PBS, and absorbance of solution was recorded after 10 min. Representative calibration curves is shown in Fig. 7b and c. The linear ranges of 0.3–20 μM and 20–8000 μM H_2O_2 were recorded with correlation coefficients of 0.9989 and 0.9906, according to A = 1.043 × [H_2O_2] (μM) + 0.0633 and A = 0.0095 × [H_2O_2] (μM), + 1.054, respectively. The detection limit (LOD) for H_2O_2 was determined to be ≈15 nM. The detection limit and the wide linear range of this biosensor are comparable to or lower than other H_2O_2 sensors (Table 1) [1,19,40–48].

The reproducibility of the HRP-rGO/Au fabrication for H_2O_2 sensing is expressed in terms of relative standard deviation (RSD), which is found to be 6.1% in PBS (2 mL, pH 7.4) containing ABTS (1 mg) and H_2O_2 (5 μL, 30%). The long-term stability of the

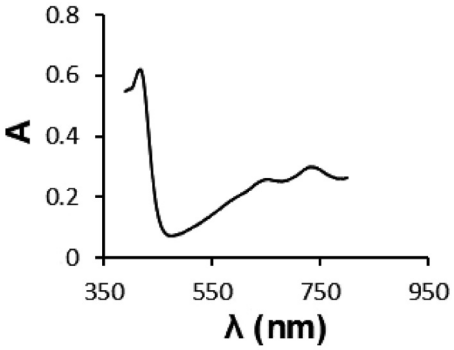

Fig. 5. The UV–Vis spectrum of ABTS (1 mg) and H_2O_2 (5 μL) in PBS (2 mL, pH 7.4) after immersion of HRP-rGO/Au for 15 min.

Table 1
Characteristics of other H_2O_2 sensing platforms.

Sensor component	Linear range (μM)	LOD (μM)	Ref.
HRP-GO	2–500	1.6	[1]
Peroxidase-Porous $CoFe_2O_4$	20–6000	20	[19]
Macroporous Silicon	10–5000	4.35	[40]
MoS_2 nanoparticles	0.005–0.1	0.002	[41]
(HRP-Pd)/ functionalized graphene	25–3500	0.05	[42]
Iodide catalyzed oxidation of TMB	0.5–1000	0.2	[43]
HRP-carbon nanotubes-polyvinyl butyral film	0.832–600	0.167	[44]
HRP-Bi-Ag nanoparticles	0.02–1	0.06	[45]
HRP–MoS_2–Graphene	0.2–1103	0.049	[46]
nafion/HRP/Ag	0.03–0.5	0.13	[47]
HRP/MWCNT	9–1000	4	[48]
HRP-rGO	0.3–20 20–8000	0.015	This work

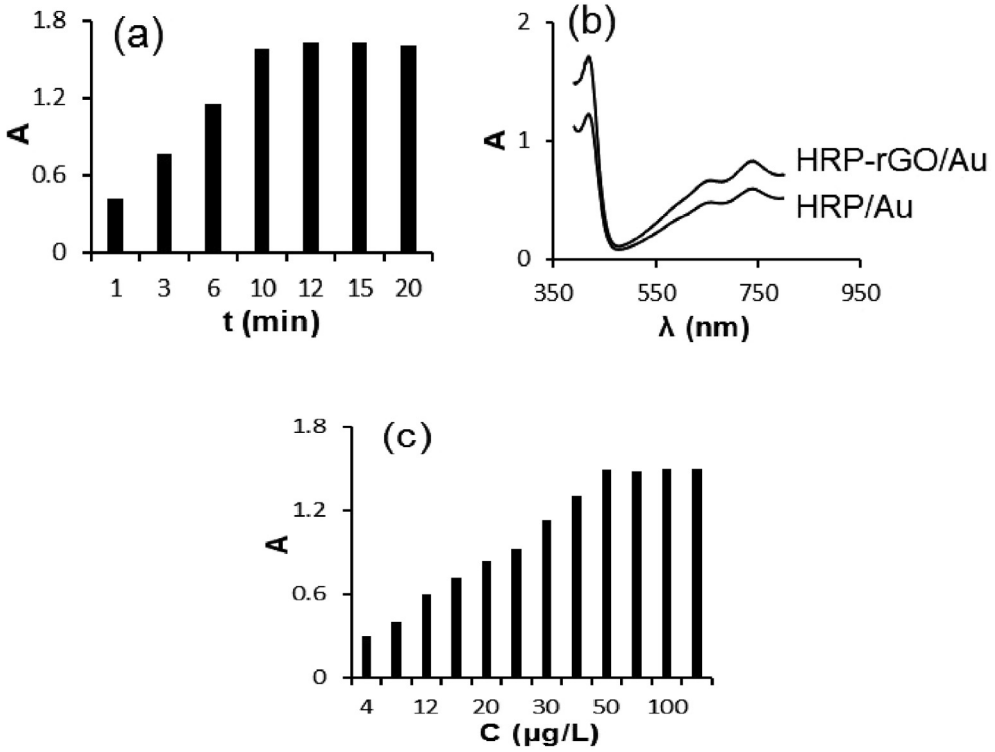

Fig. 6. (a) The time effect in catalytic reaction of ABTS (1 mg) and H_2O_2 (5 μL) in PBS (2 mL, pH 7.4) by HRP-rGO/Au; (b) The effect of rGO in catalytic reaction; (c) The HRP concentration immobilized onto rGO/Au biosensor for determination of H_2O_2.

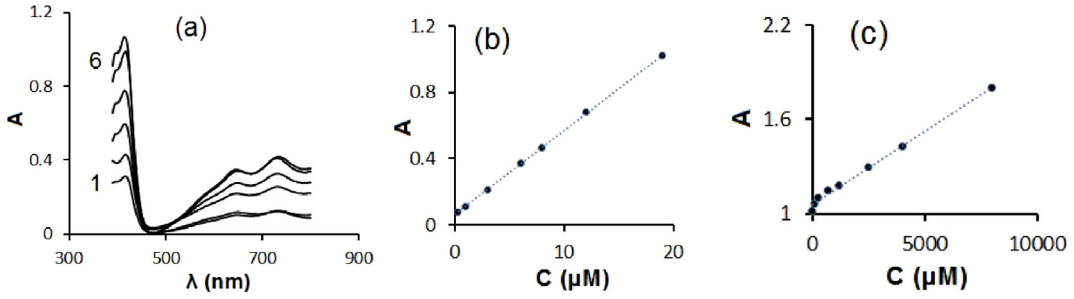

Fig. 7. (a) The UV–Vis spectra of ABTS (1 mg) in PBS (2 mL, pH 7.4) by HRP-rGO/Au with different concentrations of H_2O_2: (1) 3, (2) 6, (3) 12 (4) 16, (5) 20 and (6) 30; (b) and (c) The absorbtion plot of solution vs·H_2O_2 concentration.

Table 2
Determination of H_2O_2 in several commercial beverages using HRP-rGO/Au as biosensor.

Sample	Spiked (μM)	Found (μM)	Mean recovery (%)
Low fat milk (Kalleh)	5	5.1	102 ± 2.3
Low fat milk (Mihan)	5	4.7	94 ± 1.9
Low fat milk (Damdaran)	5	4.8	96 ± 3.7
Full fat milk (Kalleh)	8	7.6	95 ± 4.2
Full fat milk (Mihan)	8	8.1	101 ± 2.5
Orange juice (Takdaneh)	10	9.7	97 ± 5.2
Apple juice (Takdaneh)	10	9.4	94 ± 0.9

biosensor when stored at 4 °C for about 2 weeks was in addition showed loss of 7.8%.

3.4. H_2O_2 sensing in real samples

The suitability of the proposed method for testing low and full fat milks (Kalleh, Mihan and Damdaran), orange juice (Takdaneh) and apple juice (Takdaneh) was analysed using UV–Vis spectroscopy (Table 2). The accuracy of the proposed method was assessed by performing recovery experiments using the standard addition method. A known amount of H_2O_2 was added to real samples. The obtained mean recoveries and relative standard deviations were in the ranges of 94–102% and 0.9–5.2%, respectively (Table 2). The results revealed that the proposed method can accurately determine any small changes of the H_2O_2 concentration in the samples.

4. Conclusion

In this work, a cost-efficient H_2O_2 biosensor was fabricated based on immobilized HRP enzyme on rGO/Au interface with a simple and reproducible procedure. We demonstrated the quantitative and qualitative characteristics of the proposed biosensor using UV–Vis analysis. The detection limit of analysis was 15 nM. We also evaluated that the concentration of active HRP immobilized onto rGO/Au biosensor for determination of H_2O_2 corresponds to 50 μg/L. Good reproducibility and long-term stability were also displayed on the proposed biosensor. The fabricated biosensor is promising for the practical application in detection of H_2O_2 in different beverages.

Declaration of Competing Interest

The authors declare that they have no known competing financial interests or personal relationships that could have appeared to influence the work reported in this paper.

Acknowledgment

The authors are sincerely thankful for the research facilities provided by the Ayatollah Amoli Branch of the Islamic Azad University.

References

[1] Y. Wang, K.J. Zhao, Z.H. Zhang, H. Jia, J. Chen, C.H. Fu, Simple approach to fabricate a highly sensitive H_2O_2 biosensor by one-step of graphene oxide and horseradish peroxidase co-immobilized glassy carbon electrode, Int. J. Electrochem. Sci. 13 (2018) 2921–2933.
[2] Y. Tao, E.G. Ju, J.S. Ren, X.G. Qu, Poly pyrrole nanoparticles as promising enzyme mimics for sensitive hydrogen peroxide detection, Chem. Commun. 50 (2014) 3030–3032.
[3] J. Sun, C.H. Li, Y. Qi, S.H. Guo, X. Liang, Optimizing colorimetric assay based on V_2O_5 nanozymes for sensitive detection of H_2O_2 and glucose, Sensors 16 (2016) 584–595.
[4] J.S. Kumar, N. Chandra Murmu, T. Kuila, Recent trends in the graphene-based sensors for the detection of hydrogen peroxide, AIMS Mater. Sci. 5 (2018) 422–466.
[5] G. Yu, W. Wu, X. Pan, Q. Zhao, X. Wei, Q. Lu, High sensitive and selective sensing of hydrogen peroxide released from pheochromocytoma cells based on Pt-Au bimetallic nanoparticles electrodeposited on reduced graphene sheets, Sensors 15 (2015) 2709–2722.
[6] S.J. Li, L.L. Hou, M.Z. Chang, J.J. Yan, L. Liu, A novel enzyme-free hydrogen peroxide sensor based on electrode modified with gold nanoparticles-overoxidized polydopamine composites, Int. J. Electrochem. Sci. 11 (2016) 2887–2896.
[7] Q. Wang, A. Kromka, J. Houdkova, O. Babchenko, B. Rezek, M. Li, R. Boukherroub, S. Szunerits, Nanomolar hydrogen peroxide detection using horseradish peroxidase covalently linked to undoped nanocrystalline diamond surfaces, Langmuir 28 (2012) 587–592.
[8] C.C. Hsu, Y.R. Lo, Y.C. Lin, Y.C. Shi, P.L. Li, A spectrometric method for hydrogen peroxide concentration measurement with a reusable and cost-efficient sensor, Sensors 15 (2015) 25716–25729.
[9] H. Baccar, C.P. Adams, A. Abdelghani, S.O. Obare, Chronoamperometric-based detection of hydrogen peroxide using palladium nanoparticles, Int. J. Nanotechnol. 10 (2013) 563–576.
[10] D. Humer, O. Spadiut, Improving the performance of horseradish peroxidase by site directed mutagenesis, Int. J. Mol. Sci. 20 (2019) 916–930.
[11] S. Lu, J. Song, L. Campbell-Palmer, A modified chemiluminescence method for hydrogen peroxide determination in apple fruit tissues, Sci. Hortic. 120 (2009) 336–341.
[12] Y.Z. Li, A. Townshend, Evaluation of the adsorptive immobilization of horseradish peroxidase on PTFE tubing in flow systems for hydrogen peroxide determination using fluorescence detection, Anal. Chim. Acta 359 (1998) 149–156.
[13] J.R. Xu, Z.M. Chen, Determination of peroxides in environmental samples by high performance liquid chromatography, Chin. J. Chromatogr. 23 (2005) 366–369.
[14] C.H. Wang, C. Yang, Y.Y. Song, W. Gao, X.H. Xia, Adsorption and direct electron transfer from hemoglobin into a three-dimensionally ordered macroporous gold film, Adv. Funct. Mater. 15 (2005) 1267–1275.
[15] N.V. Klassen, D. Marchington, H.C.E. McGowan, H_2O_2 determination by the I3-method and by $KMnO_4$ titration, Anal. Chem. 66 (1994) 2921–2925.
[16] A.E. Albers, V.S. Okreglak, C.J. Chang, AFRET-based approach to ratiometric fluorescence detection of hydrogen peroxide, J. Am. Chem. Soc. 128 (2006) 9640–9641.
[17] F. He, Y. Tang, M. Yu, S. Wang, Y. Li, D. Zhu, Fluorescence amplifying detection of hydrogen peroxide with cationic conjugated polymers, and its application to glucose sensing, Adv. Funct. Mater. 16 (2006) 91–94.
[18] K. Sunil, B. Narayana, Spectrophotometric determination of hydrogen peroxide in water and cream samples, Bull. Environ. Contam. Toxicol. 81 (2008) 422–426.
[19] L. Wu, G. Wan, N. Hu, Z.h. He, S.h. Shi, Y. Suo, K. Wang, X. Xu, Y. Tang, G. Wang, Synthesis of porous $CoFe_2O_4$ and Its application as a peroxidase mimetic for colorimetric detection of H_2O_2 and organic pollutant degradation, Nanomater. 8 (2018) 451–466.
[20] X. Cheng, L. Challier, A. Etcheberry, V. Noël, H. Perez, The ABTS-HRP system as an alternative method to RRDE for the determination of the selectivity of the oxygen reduction reaction, Int. J. Electrochem. Sci. 7 (2012) 6247–6264.
[21] E.N. Kadnikova, N.M. Kostic, Oxidation of ABTS by hydrogen peroxide catalyzed by horseradish peroxidase encapsulated into sol–gel glass: Effects of glass matrix on reactivity, J. Mol. Catal. B: Enzym. 18 (2002) 39–48.
[22] J. Zdarta, A.S. Meyer, T. Jesionowski, M. Pinelo, A General overview of support Materials for enzyme immobilization: characteristics, properties, practical utility, Catal. 8 (2018) 92–118.
[23] Z.J. Wang, M.Y. Li, P.P. Su, Y.J. Zhang, Y.F. Shen, D.X. Han, A. Ivaska, L. Niu, Direct electron transfer of horseradish peroxidase and its electrocatalysis based on carbon nanotube/thionine/gold composites, Electrochem. Commun. 10 (2008) 306–310.
[24] H. Shi, Y. Yang, J. Huang, Z. Zhao, X. Xu, J. Anzai, T. Osa, Q. Chen, Amperometric choline biosensors prepared by layer-by-layer deposition of choline oxidase on the Prussian blue-modified platinum electrode, Talanta 70 (2006) 852–858.
[25] Y. Wang, Y. Hasebe, Carbon felt-based bioelectrocatalytic flow-through detectors: Highly sensitive amperometric determination of H_2O_2 based on a direct electrochemistry of covalently modified horseradish peroxidase using cyanuric chloride as a linking agent, Sens. Actuators B 155 (2011) 722–729.
[26] F. Chekin, W. Myshin, R. Ye, S. Mellinte, S. Singh, S. Kurungot, R. Boukherrub, S. Szunerits, Graphene-modified electrodes for sensing doxorubicin hydrochloride in human plasma, Anal. Bioanal. Chem. 411 (2019) 1509–1516.
[27] H. Bagheri Ladmakhi, F. Chekin, J.B. Raoof, S.h. Fathi, Electrochemical sensor based on magnetite graphene oxide/ordered mesoporous carbon hybrid to detection of allopurinol in clinical samples, Talanta 211 (2020) 120759.
[28] E. Vatandost, A. Ghorbani-HasanSaraei, F. Chekin, S.h. Naghizadeh Raeisi, S.A. Shahidi, Antioxidant, antibacterial and anticancer performance of reduced graphene oxide prepared via green tea extract assisted biosynthesis, Chem. Select 5 (2020) 10401–10406.
[29] N. Samimi Tehrani, M. Masoumi, F. Chekin, M. Sharifzadeh Baei, Nitrogen doped porous reduced graphene oxide hybrid as a nanocarrier of imatinib anticancer drug, Russ. J. Appl. Chem. 93 (2020) 1221–1228.
[30] I.V. Pavlidis, M. Patila, U.T. Bornscheuer, D. Gournis, H. Stamatis, Graphene-based nanobiocatalytic systems: recent advances and future prospects, Trends Biotechnol. 32 (2014) 312–320.

[31] J. Liu, Z. Liu, C.J. Barrow, W. Yang, Molecularly engineered graphene surfaces for sensing applications: a review, Anal. Chim. Acta 859 (2015) 1–19.
[32] P. Liang, H. Bao, J. Yang, L. Zhang, G. Chen, Preparation of porous graphene oxide–poly (urea–formaldehyde) hybrid monolith for trypsin immobilization and efficient proteolysis, Carbon 97 (2016) 25–34.
[33] A.S. Campbell, C. Dong, F. Meng, J. Hardinger, G. Perhinschi, N. Wu, et al., Enzyme catalytic efficiency: a function of bio–nanointerface reactions, ACS Appl. Mater. Interfaces 6 (2014) 5393–5403.
[34] F. Chekin, R. Boukherroub, S. Szunerits, MoS_2/reduced graphene oxide nanocomposite for sensitive sensing of cysteamine in presence of uric acid in human plasma, Mater. Sci. Eng. C 73 (2017) 627–632.
[35] V.C. Sanchez, A. Jachak, R.H. Hurt, A.B. Kane, Biological interactions of graphene-family nanomaterials: an interdisciplinary review, Chem. Res. Toxicol. 25 (2012) 15–34.
[36] X. Yang, C. Zhao, E. Ju, J. Ren, X. Qu, Contrasting modulation of enzyme activity exhibited by graphene oxide and reduced graphene, Chem. Commun. 49 (2013) 8611.
[37] E. Vatandost, A. Ghorbani-HasanSaraei, F. Chekin, Sh. Naghizadeh Raeisi, S.A. Shahidi, Green tea extract assisted green synthesis of reduced graphene oxide: Application for highly sensitive electrochemical detection of sunset yellow in food products, Food Chem. X 6 (2020) 100085.
[38] Sh. Nikkhah, H. Tahermansouri, F. Chekin, Synthesis, characterization, and electrochemical properties of the modified graphene oxide with 4,4′-methylenedianiline, Mater. Lett. 211 (2018) 323–327.
[39] N. Hazhir, F. Chekin, J.B. Raoof, Sh. Fathi, A porous reduced graphene oxide/chitosan-based nanocarrier as a delivery system of doxorubicin, RSC Adv. 9 (2019) 30729–30735.
[40] N.H. Al-Hardan, M.A. Abdul Hamid, R. Shamsudin, E.M. AL-Khalqi, L.K. Keng, N. M. Ahmed, Electrochemical hydrogen peroxide sensor based on macroporous silicon, Sensors 18 (2018) 716–724.
[41] T. Wang, H. Zhu, J. Zhuo, Z. Zhu, P. Papakonstantinou, G. Lubarsky, J. Lin, M. Li, Biosensor based on ultrasmall MoS2 nanoparticles for electrochemical detection of H_2O_2 released by cells at the nanomolar level, Anal. Chem. 85 (2013) 10289–10295.
[42] S. Nandini, S. Nalini, R. Manjunatha, S. Shanmugam, J.S. Melo, G.S. Suresh, Electrochemical biosensor for the selective determination of hydrogen peroxide based on the co-deposition of palladium, horseradish peroxidase on functionalized-graphene modified graphite electrode as composite, J. Electroanal. Chem. 689 (2013) 233–242.
[43] J. Zhang, J. Peng, L. Zhu, Ch. Lai, H. Wang, W. Zou, H. Li, An easy and cost-effective colorimetric assay of hydrogen peroxide based on iodide-catalyzed oxidation of 3,3,5,5-tetramethylbenzidine, Int. J. Clin. Exp. Med. 11 (2018) 13100–13107.
[44] L. Han, H. Tao, M. Huang, Y. Zhang, Sh. Qiao, R. Shi, A hydrogen peroxide biosensor based on multiwalled carbon nanotubes-polyvinyl butyral film modified electrode, Russ. J. Electrochem. 52 (2016) 115–122.
[45] Ch. van der Horst, B. Silwana, E. Iwuoha, V. Somerset, Electrocatalytic evaluation of a horseradish peroxidase biosensor based on a novel Bi-Ag bimetallic nanocomposite, Proc. Technol. 27 (2017) 179–182.
[46] H. Song, Y. Ni, S. Kokot, Investigations of an electrochemical platform based on the layered MoS_2–graphene and horseradish peroxidase nanocomposite for direct electrochemistry and electrocatalysis, Biosens. Bioelectron. 56 (2014) 137–143.
[47] A.S. Rad, M. Jahanshahi, M. Ardjmand, A.A. Safekordi, Hydrogen peroxide biosensor based on enzymatic modification of electrode using deposited silver nano layer, Inter. J. Electrochem. Sci. 7 (2012) 2623–2632.
[48] M. Moyo, J.O. Okonkwo, N.M. Agye, A novel hydrogen peroxide biosensor based on adsorption of horseradish peroxidase onto a nanobiomaterial composite modified glassy carbon electrode, Electroanal. 25 (2013) 1946–1954.